Equivalency of Continuation and Optimization Methods to Determine Saddle-node and Limit-induced Bifurcations in Power Systems

Rafael J. Avalos, *Student Member, IEEE*, Claudio A. Cañizares, *Fellow, IEEE*, Federico Milano, *Member, IEEE*, Antonio J. Conejo, *Fellow, IEEE*

***Abstract*— This paper presents a comprehensive and detailed study of an optimization-based approach to identify and analyze saddle-node bifurcations (SNB) and limit-induced bifurcations (LIB) of a power system model, which are known to be directly associated with voltage stability problems in these systems. Theoretical studies are presented, formally demonstrating that solution points obtained from an optimization model, which is based on complementarity constraints used to properly represent generators' voltage controls, correspond to either SNB or LIB points of this model. These studies are accomplished by proving that optimality conditions of these solution points yield the transversality conditions of the corresponding bifurcation points. A simple but realistic test system is used to numerically illustrate the theoretical discussions.**

***Index Terms*— Saddle-node bifurcations, limit-induced bifurcations, transversality conditions, optimization methods, voltage stability, maximum loadability.**

I. Nomenclature

A. Variables

$x \in \mathbb{R}^{n_x}$: Vector of state variables.
$y \in \mathbb{R}^{n_y}$: Vector of algebraic variables.
$z = (x, y) \in \mathbb{R}^{n_z}$: Vector of state and algebraic variables.
$\hat{z} = (\tilde{z}, \hat{r}) \in \mathbb{R}^{n_{\hat{z}}}$: Vector of voltages and angles at all buses, and reactive power at generation buses, $\hat{z} \subset z$.
$\tilde{z} \in \mathbb{R}^{n_{\tilde{z}}}$: Vector of voltages and angles at all buses, $\tilde{z} \subset \hat{z}$.
$\hat{r} \in \mathbb{R}^{n_{\hat{r}}}$: Vector of actuation limit variables, i.e. reactive power generation in this paper.
$\lambda \in \mathbb{R}^{+}$: Loading factor.
$p \in \mathbb{R}^{n_p}$: Vector of controllable parameters associated with control settings.
$\hat{p} \in \mathbb{R}^{n_{\hat{p}}}$: Vector of generation voltage levels and base active power injections, $\hat{p} \subseteq p$.
$\hat{\mu}$: Vector of Lagrange multipliers.
$\hat{v}$: Normalized zero right eigenvector.
$\hat{w}$: Normalized zero left eigenvector.

This research was partially supported by grants from NSERC, Canada, and the Ministry of Education and Science, Spain.

R. J. Avalos and C. Cañizares are with the Department of Electrical and Computer Engineering, University of Waterloo, Waterloo, Ontario, N2L 3G1, Canada (email: ccanizar@uwaterloo.ca).

F. Milano and A. J. Conejo are with the Department of Electrical Engineering, Universidad de Castilla-La Mancha, Campus Universitario s/n, 13071 Ciudad Real, Spain (email: Antonio.Conejo@uclm.es).

B. Functions

$f(\cdot) : \mathbb{R}^{n_x} \times \mathbb{R}^{n_y} \times \mathbb{R}^{+} \times \mathbb{R}^{n_p} \mapsto \mathbb{R}^{n_x}$: Nonlinear vector field associated with the state variables.
$g(\cdot) : \mathbb{R}^{n_x} \times \mathbb{R}^{n_y} \times \mathbb{R}^{+} \times \mathbb{R}^{n_p} \mapsto \mathbb{R}^{n_y}$: Nonlinear algebraic constraints.
$F(\cdot) = (f(\cdot), g(\cdot)) : \mathbb{R}^{n_z} \times \mathbb{R}^{+} \times \mathbb{R}^{n_p} \mapsto \mathbb{R}^{n_z}$: Nonlinear differential-algebraic power system model.
$G(\cdot) : \mathbb{R}^{n_{\hat{z}}} \times \mathbb{R}^{+} \times \mathbb{R}^{n_{\hat{p}}} \mapsto \mathbb{R}^{n_{\hat{z}}}$: Standard power flow equations (2 equations per bus), $G \subset g$.
$\hat{g}(\cdot) : \mathbb{R}^{n_{\tilde{z}}} \times \mathbb{R}^{n_{\hat{r}}} \times \mathbb{R}^{+} \times \mathbb{R}^{n_{\hat{p}}} \mapsto \mathbb{R}^{n_{\tilde{z}}}$: Power flow equations that do not include actuation limit equations, $\hat{g} \subset G$.
$\hat{s}(\cdot) : \mathbb{R}^{n_{\tilde{z}}} \times \mathbb{R}^{n_{\hat{r}}} \times \mathbb{R}^{+} \times \mathbb{R}^{n_{\hat{p}}} \mapsto \mathbb{R}^{n_{\hat{r}}}$: Actuation limit functions, i.e. nonlinear functions of the generator reactive power flow equations, $\hat{s} \subset G$.
$\hat{h}(\cdot) : \mathbb{R}^{n_{\tilde{z}}} \times \mathbb{R}^{n_{\hat{r}}} \times \mathbb{R}^{+} \times \mathbb{R}^{n_{\hat{p}}} \mapsto \mathbb{R}^{n_{\hat{r}}}$: All actuation limit equations, $\hat{s} \subset \hat{h}$.

C. Subscripts

o: denotes equilibrium/initial point.
c: denotes bifurcation/optimal point.

II. Introduction

VOLTAGE stability (VS) has become rather important in modern power systems, due to the fact that systems are being operated close to their VS limits, as demonstrated by many recent major blackouts which can be directly associated with VS problems. Furthermore, the implementation and application of open market principles have exacerbated this problem, since security margins are being reduced to respond to market pressures [1]–[3]. Consequently, the prediction, identification and avoidance of voltage instability points play a significant role in power system planning and operation. Nonlinear phenomena, particularly saddle-node bifurcations (SNB) and limit-induced bifurcations (LIB) have been shown to be directly associated with VS problems in power systems [4], and are hence the main concern in the current paper. It is important to highlight the fact that other types of bifurcations in power systems, such as Hopf bifurcations (HB), associated with oscillatory instabilities [5], and Singularity-induced bifurcations (SIB), associated with differential-algebraic models [4], [6], [7], are not considered in this paper, since these

types of bifurcations have not been shown in practice to be directly related to VS problems [4].

Continuation Power Flow (CPF) and Optimal-Power-Flow-based Direct Methods (OPF-DM) are two different techniques that are used in practice to compute VS margins. The most widely used method is the CPF, which is a technique that consists in increasing the loading level until a voltage, current or voltage stability limit is detected in a power flow model, and it is based on a predictor-corrector scheme to find the complete equilibrium profile or bifurcation manifold (PV curve) of a set of power flow equations with respect to a given scalar variable. This scalar parameter is typically referred to as the bifurcation parameter or loading factor, as it is used to model changes in system demand [8], [9]. In [10], it is shown that this method can be viewed as a Generalized Reduced Gradient (GRG) approach for solving a maximum loadability optimization problem.

The OPF-DM is an optimization-based method that consists in maximizing the loading factor, while satisfying the power flow equations, bus-voltage and generators' reactive power limits, and other operating limits of interest (e.g. transmission-line thermal limits) [11], [12]. A variety of OPF models based on this problem definition have been proposed; for example, the authors in [13]–[15] propose a multi-objective OPF for maximizing both the social welfare and the loading factor. This type of optimization problems can be solved by means of Interior-Point Methods (IPM), which have been shown to be computationally efficient for power system studies [16].

An important difference between the CPF and the most popular implementations of the OPF-DM is that, in the CPF, the voltage is kept constant at generation buses while their reactive power output is within limits (PV bus model). In the "standard" OPF-DM, generator voltages and reactive powers are allowed to change within limits, so that "optimal" operating conditions are obtained. These different approaches may lead to different solutions; an interesting discussion about this issue can be found in [2]. An OPF-DM model that is shown empirically to produce similar results to the CPF approach is presented and discussed in [17], where PV buses are modeled using complementarity constraints; the latter are shown here to be particularly important to demonstrate the equivalency of CPF and OPF-DM approaches.

The current paper presents a detailed theoretical analysis of the application of OPF-DM to the study of SNBs and LIBs in power systems. Previous works have formally shown that optimization methods can be used to compute SNBs in power system models, and that these methods are basically equivalent to more "classical" computational approaches [10]. Also, some issues associated with the application of OPF-DMs to the computation of LIBs are discussed in [18], and the structure of the loadability surface is studied in [19] using similar optimization methods. In [20], fold bifurcations are also studied based on an optimization model. However, up to now, to the authors' knowledge, the links between solutions of OPF-DMs and SNBs and LIBs have not yet been dealt with in the technical literature as formally and systematically as it is done here. Hence, the present paper concentrates on demonstrating that solution points obtained from a given OPF-DM model correspond to either SNB or LIB points; this is accomplished by showing that the optimality conditions of these solution points yield the transversality conditions of the corresponding bifurcation points. A simple but realistic test system example is used to numerically illustrate the presented theoretical discussions.

This paper is structured as follows: Section III presents a concise but thorough description of the VS problem, the power system model used to study it, and its mathematical characterization through bifurcation theory. The optimization models used for the OPF-DM studies of interest to this paper are discussed in detail in Section IV. Section V concentrates on formally showing that the solution points of an optimization model described in the previous section correspond to either SNB or LIB points, based on optimality conditions and the corresponding bifurcation transversality conditions. The theoretical discussions are illustrated with the help of a 6-bus test system in Section VI. Finally, in Section VII, the main contributions of the paper are highlighted.

III. Definitions

Voltage stability is associated with the capability of a power system to maintain steady acceptable voltages at all buses, not only under normal operating conditions, but also after being subjected to a disturbance [21]. It is a well established fact that voltage collapse in power systems is associated with system demand increasing beyond certain limits, as well as with the lack or reactive power support in the system caused by limitations in the generation or transmission of reactive power. System contingencies such as generator or line unexpected outages exacerbate, if not trigger, the VS problems [4], [22]. Usually, VS analysis consist in determining the system conditions at which the equilibrium points of a dynamic model of the power system merge and disappear; these points have been associated with certain bifurcations of the corresponding system models [4].

A. System Models

Power systems are typically modeled with nonlinear differential-algebraic equations (DAE), which are a class of nonlinear systems, as follows:

$$\left[\begin{array}{c}\dot{x}\\0\end{array}\right]=\left[\begin{array}{c}f(x,y,\lambda,p)\\g(x,y,\lambda,p)\end{array}\right]=F(z,\lambda,p) \tag{1}$$

where $x \in \mathbb{R}^{n_x}$ is a vector of the state variables which represents the dynamic states of generators, loads and system controllers; $y \in \mathbb{R}^{n_y}$ is a vector of algebraic variables that typically results from neglecting fast dynamics, such as load bus voltages magnitudes and angles; $z = (x, y) \in \mathbb{R}^{n_z}$; $\lambda \in \mathbb{R}^{+}$ stands for a slow varying "uncontrollable" parameter, typically used to represent load changes that move the system from one equilibrium point to another; and $p \in \mathbb{R}^{n_p}$ represents "controllable" parameters associated with control settings, such as Automatic Voltage Regulator (AVR) set points. The function $f : \mathbb{R}^{n_x} \times \mathbb{R}^{n_y} \times \mathbb{R}^{+} \times \mathbb{R}^{n_p} \mapsto \mathbb{R}^{n_x}$ is a nonlinear vector field directly associated with the state variables x, and representing the system differential equations, such as those

associated with the generator mechanical dynamics; and $g : \mathbb{R}^{n_x} \times \mathbb{R}^{n_y} \times \mathbb{R}^{+} \times \mathbb{R}^{n_p} \mapsto \mathbb{R}^{n_y}$ represents the system nonlinear algebraic constraints, such as the power flow equations, and algebraic constraints associated with the synchronous machine model.

If the Jacobian $\nabla_y^T g(\cdot)$ of the algebraic constraints is invertible, i.e. nonsingular along a "solution path" of (1), the behavior of the system is mainly defined by the following Ordinary Differential Equation (ODE) model

$$\dot{x} = f(x, y^{-1}(x, \lambda, p), \lambda, p)$$

were $y^{-1}(x, \lambda, p)$ results from applying the Implicit Function Theorem to the algebraic constraints along the system trajectories of interest [10], [23]. The interested reader is referred to [24] for a detailed discussion when $\nabla_y^T g(\cdot)$ is not guaranteed to be invertible; this problem is associated with SIBs, which are beyond the scope of the present paper, since this phenomenon is not directly related to VS problems in practice [4].

Equilibrium points $z_o = (x_o, y_o)$ of (1) are defined by the solutions of the nonlinear equations:

$$F(z_o, \lambda_o, p_o) = \begin{bmatrix} f(x_o, y_o, \lambda_o, p_o) \\ g(x_o, y_o, \lambda_o, p_o) \end{bmatrix} = 0$$

It is important to highlight the fact that the system equilibria are in practice obtained from a subset of equations:

$$G(\hat{z}_o, \lambda_o, \hat{p}_o) = G|_o = 0 \subset F(z_o, \lambda_o, p_o) = F|_o = 0 \quad (2)$$

where $G|_o = 0$ stands for the power flow equations, with $G \subset g$; $\hat{z}_o \in \mathbb{R}^{n_{\hat{z}}} \subset z$ is the set of voltage and angles at all buses as well as the reactive power of the generator (PV) buses; and $\hat{p}_o \in \mathbb{R}^{n_{\hat{p}}} \subseteq p$ usually represents the voltage levels and "base" active power injections at PV buses, "base" active and reactive power injections at load buses, transformer fixed-tap settings and other controller settings.

Power flow models have been used in practice for voltage collapse studies, since these models form the basis for defining the actual system operating conditions [4]. However, one should be aware that the solutions of the power flow equations do not necessarily correspond to system equilibria, since a solution of $G|_o = 0$ does not imply that $F|_o = 0$, even though this is not a significant issue in practice. Therefore, in this paper, actual SNBs and LIBs of (1) are assumed to correspond to similar "bifurcation" points of the power flow equations, which is the case of certain power system models [25], [26]; thus, the paper concentrates on the analysis of SNBs and LIBs of (2).

B. Bifurcation Analysis

Bifurcation theory yields tools that are able to classify, study, and give qualitative and quantitative information about the behavior of a nonlinear system close to bifurcation or "critical" equilibrium points as system parameters change [27]. The parameters are assumed to change "slowly", so that the system can be assumed to "move" from one equilibrium point to another with these changes (quasi-static assumption). Hence, bifurcation analysis is usually associated with the study of equilibria of the nonlinear system model [4].

In power systems, SNBs and some types of LIBs are basically characterized by the local merging and disappearance of power flow solutions as certain system parameters, particularly system demand, slowly change; this phenomenon has been associated with VS problems [4]. These kinds of bifurcations are also referred to in the technical literature as fold or turning points.

1) Saddle-Node Bifurcations (SNB): These types of codimension-1 (single parameter), generic bifurcations occur when two equilibrium points, typically one stable and one unstable in practice, merge and disappear as the parameter λ slowly changes, as illustrated in the PV curves of Figs. 1(a) and 1(b), where V_{G_i} and Q_{G_i} stand for a generator i's terminal voltage magnitude and reactive power, respectively. Mathematically, the SNB point for the power flow model (2) is a solution point $(\hat{z}_c, \lambda_c, \hat{p}_o)$ where the Jacobian $\nabla_{\hat{z}}^T G|_c$ has a simple zero eigenvalue, with nonzero eigenvectors [26], [28]. The following *transversality conditions* can be used to characterize and detect SNBs [10]:

$$\nabla_{\hat{z}}^T G|_c \hat{v} = \nabla_{\hat{z}} G|_c \hat{w} = 0 \quad (3)$$

$$\nabla_{\lambda} G|_c \; \hat{w} \neq 0 \quad (4)$$

$$\hat{w}^T \left[\nabla_{\hat{z}}^{2^T} G|_c \hat{v} \right] \hat{v} \neq 0 \quad (5)$$

where $\hat{v}$ and $\hat{w} \in \mathbb{R}^{n_{\hat{z}}}$ are normalized right and left eigenvectors of the Jacobian $\nabla_{\hat{z}}^T G|_c$. The first condition implies that the Jacobian matrix is singular; the second and third conditions ensure that there are no equilibria near $(\hat{z}_c, \lambda_c, \hat{p}_o)$ for $\lambda > \lambda_c$ (or $\lambda < \lambda_c$, depending on the sign of (5)). Note that the subscript c is used throughout the paper to denote a bifurcation point.

2) Limit-Induced Bifurcations (LIB): These types of codimension-1 (single parameter), generic bifurcations in power systems were first studied in detail in [29], and can be typically encountered in these systems, since as the load increases, reactive power demand generally increases as well, and thus reactive power limits of generators or other voltage regulating devices are reached. These bifurcations result in reduced VS margins, and in some cases the operating point "disappears" causing a voltage collapse [4], as illustrated in Fig. 1. Mathematically, the LIBs associated with power flow models are solution points $(\hat{z}_c, \lambda_c, \hat{p}_o)$ where all the eigenvalues of the corresponding Jacobian $\nabla_{\hat{z}}^T G|_c$ have nonzero real parts, i.e. the power flow Jacobian is nonsingular [30].

These bifurcations are divided into two types, namely, limit-induced dynamic bifurcations (LIDB), and limit-induced static bifurcations (LISB). In the case of LIDBs, the equilibrium points continue to exist after being reached as the bifurcation parameter λ changes, as illustrated in Figs. 1(b) and 1(d). On the other hand, LISBs are somewhat similar to SNBs in the sense that these correspond to points at which two solutions merge and disappear as the bifurcation parameter λ changes, as depicted in Fig. 1(c); thus, LISBs also are associated with maximum loadability margins in power flow models.

In general, the limits that trigger LIBs can be categorized into three basic types of limits, namely, actuation limits, state

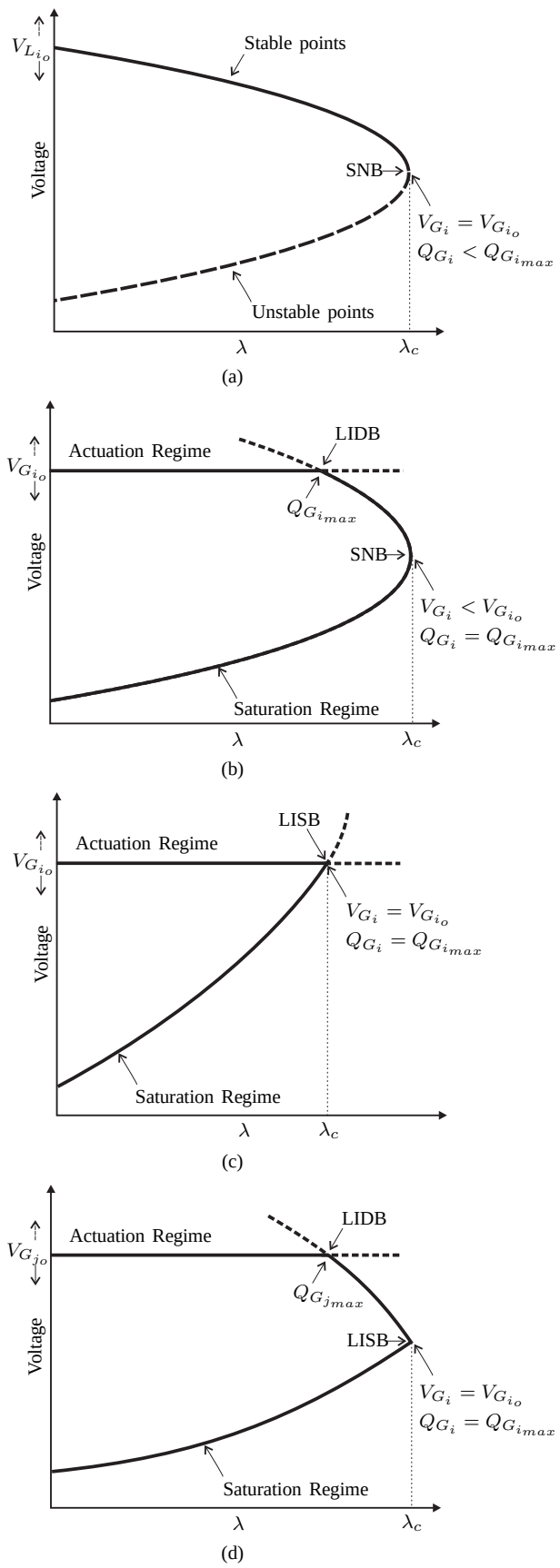

Fig. 1. Main bifurcations observed in PV curves: (a) SNB without Q_G limits; (b) LIDB followed by an SNB; (c) LISB; (d) LISB preceded by an LIDB.

limits and switching limits [30]. The actuation limits appear when certain variables, which are functions of some of the state variables encounter a limit. These limits do not directly affect the state variables but the overall dynamics, and can be modeled through the use of actuation functions. In power systems models, actuation limits typically depend on only one state variable at a time, and one of these inequalities becomes an equality on encountering a limit. The state limits have a direct effect on the state variables, and occur when a state reaches its limit, which results in the system dimension dropping by one, since the state variable becomes a constant in the model. These kinds of limits can be modeled by setting the state derivative equal to zero when the limits are reached. Finally, the switching limits are followed by pre-established actions (e.g. relaying mechanisms or protective limiters in the physical system) that might result in a change in the whole system, and consequently in the states. These limits can be modeled, for instance, by introducing certain binary variables that represent the internal logic of a relay element.

For the power flow model, actuation limits can be directly associated with LIBs. Therefore, this paper focuses on these types of limits to analyze LIBs, using the following representation that results from the proper ordering of the power flow equations (2), and with similar notation to the one proposed in [30]:

$$G(\hat{z}, \lambda, \hat{p}) = \begin{bmatrix} \hat{g}(\tilde{z}, \hat{r}, \lambda, \hat{p}) \\ \hat{r} - \hat{s}(\tilde{z}, \lambda, \hat{p}) \end{bmatrix} = 0 \tag{6}$$

where $\tilde{z} \in \mathbb{R}^{n_{\tilde{z}}}$, $\hat{r} \in \mathbb{R}^{n_{\hat{r}}}$, $\hat{z} = (\tilde{z}, \hat{r})$, and the actuation limits are modeled as:

$$\hat{r}_i = \begin{cases} \hat{r}_{i_{min}}, & \text{if } \hat{s}_i(\tilde{z}, \lambda, \hat{p}) < \hat{r}_{i_{min}} \\ \hat{s}_i(\tilde{z}, \lambda, \hat{p}), & \text{if } \hat{r}_{i_{min}} \leq \hat{s}_i(\tilde{z}, \lambda, \hat{p}) \leq \hat{r}_{i_{max}} \\ \hat{r}_{i_{max}}, & \text{if } \hat{s}_i(\tilde{z}, \lambda, \hat{p}) > \hat{r}_{i_{max}} \end{cases} \tag{7}$$

Since in power flow models, LIBs of interest are typically associated with generators reaching their maximum reactive power limits, at an LIB point $(\hat{z}_c, \lambda_c, \hat{p}_o) = (\tilde{z}_c, \hat{r}_c, \lambda_c, \hat{p}_o)$, the following two sets of equations apply:

$$G_a(\hat{z}_c, \lambda_c, \hat{p}_o) = \begin{bmatrix} \hat{g}(\tilde{z}_c, \hat{r}_c, \lambda_c, \hat{p}_o) \\ \hat{r}_{k_c} - \hat{s}_k(\tilde{z}_c, \lambda_c, \hat{p}_o) \quad \forall k \neq i \\ \hat{r}_{i_c} - \hat{s}_i(\tilde{z}_c, \lambda_c, \hat{p}_o) \end{bmatrix} = 0 \tag{8}$$

$$G_b(\hat{z}_c, \lambda_c, \hat{p}_o) = \begin{bmatrix} \hat{g}(\tilde{z}_c, \hat{r}_c, \lambda_c, \hat{p}_o) \\ \hat{r}_{k_c} - \hat{s}_k(\tilde{z}_c, \lambda_c, \hat{p}_o) \quad \forall k \neq i \\ \hat{r}_{i_c} - \hat{r}_{i_{max}} \end{bmatrix} = 0 \tag{9}$$

where (8) corresponds to the system equations "before" a limit is reached, and (9) represents the system "after" a limit is reached as λ increases. These system conditions can be referred to as the system in actuation regime and in saturation regime, respectively, as depicted in Fig. 1. Notice that a "critical" solution or bifurcation point must satisfy both sets of equations, and that the difference between (8) and (9) is only the equation corresponding to actuation limit i, since an LIB occurs when a single generator i reaches its maximum reactive power limit.

The transversality conditions for LIBs may then be defined as follows [30]:

1) $G_a|_c = G_b|_c = 0$
2) Jacobians $J_a^i = \nabla_{\hat{z}}^T G_a|_c$ and $J_b^i = \nabla_{\hat{z}}^T G_b|_c$ have nonzero real parts, i.e.

$$\det(J_a^i) \neq 0 \quad \text{and} \quad \det(J_b^i) \neq 0 \tag{10}$$

3) The index:

$$\alpha = \frac{\det J_a^i}{\det J_b^i} \neq 0 \tag{11}$$

defines the type of LIB; thus, $\alpha > 0$ for an LISB, and $\alpha < 0$ for an LIDB.

IV. OPF-based Direct Method (OPF-DM)

Optimization methods may be used to compute maximum loadability points of power flow models, which are directly associated with SNBs and LISBs of the corresponding model equations, as initially proposed in [11]. Thus, based on the aforementioned SNB and LIB definitions, the bifurcation point directly corresponds to the solution of the following optimization model, as formally demonstrated in Section V:

$$\max_{\tilde{z},\hat{r},\lambda} \quad \lambda \tag{12a}$$
$$\text{s.t.} \quad \hat{g}(\tilde{z},\hat{r},\lambda,\hat{p}_o) = 0 \tag{12b}$$
$$\hat{h}(\tilde{z},\hat{r},\lambda,\hat{p}_o) = 0 \tag{12c}$$
$$\hat{r}_{min} \leq \hat{r} \leq \hat{r}_{max} \tag{12d}$$

where the nonlinear function $\hat{h}$ is used to represent the actuation limit equations introduced in (6), since in these optimization models, the actuation limits are typically not represented explicitly, as illustrated below. The issue of how constraints (12c) are actually represented in this model, and the effect of this modeling on the solution of optimization problem (12) is discussed in detail below. Note that (12d) basically corresponds to (7).

A. OPF-DM in Standard Form

For a typical power flow model, let $\tilde{z} = (\delta, V_L, K_G)$, $\hat{r} = (Q_G, V_G)$, and $\hat{p} = (P_S, P_D)$. In this case, δ stands for all the bus voltage phasor angles but one (slack bus); V_L and V_G correspond to the load and generator bus voltage phasor magnitudes, respectively; and Q_G represents the generator reactive power output. The variables P_S and P_D define the change in generation and demand powers, respectively, as follows:

$$\begin{aligned} P_G &= P_{G_o} + (\lambda + K_G) P_S \\ P_L &= P_{L_o} + \lambda\, P_D \\ Q_L &= Q_{L_o} + \lambda\, K_L P_D \end{aligned} \tag{13}$$

where P_{G_o}, P_{L_o} and Q_{L_o} stand for the "base" generation and load levels, thus defining an "initial" operating point; K_G is a variable used to model a distributed slack bus; and K_L is a constant used to represent a constant power factor load.

Based on the aforementioned variable definition and if the actuation functions (12c) are omitted, the model can be restated as:

$$\max_{\substack{\delta,V_L,K_G \\ Q_G,V_G,\lambda}} \quad \lambda \tag{14a}$$
$$\text{s.t.} \quad G(\delta, V_L, K_G, Q_G, V_G, \lambda, P_S, P_D) = 0 \tag{14b}$$
$$Q_{G_{i_{min}}} \leq Q_{G_i} \leq Q_{G_{i_{max}}} \quad \forall i \in \mathcal{G} \tag{14c}$$
$$V_{G_{i_{min}}} \leq V_{G_i} \leq V_{G_{i_{max}}} \quad \forall i \in \mathcal{G} \tag{14d}$$

where $\mathcal{G}$ is the set of generation buses. It is important to highlight the fact that in this optimization model no other limits such as load bus voltage magnitude limits, generator active power limits, or power transfer limits, which are typical operating limits considered in such OPF models, are represented in this model. The reason for this is that these are "hard" limits and not actuation limits, i.e. limits that basically define "undesirable" operating conditions which may be associated with system protections rather than system controls, and hence do not lead to LIBs. Thus, these limits would only clutter the theoretical analyzes presented in the next section, without adding much to the discussions.

It has been shown that if no limits become active, the Karush-Kuhn-Tucker (KKT) optimality conditions evaluated at the solution point of (14) are equivalent to the transversality conditions (3) and (4) for SNBs [10]; however, it has not yet been formally shown for these particular types of bifurcations that the third transversality condition (5) is also met, which is an issue addressed here. It can also be argued that this model may provide a different maximum loading point different from that obtained using the CPF technique if reactive power limits become active [17]. The main problem is that (14) does not include a proper representation of PV buses, and hence there is no guarantee that the voltage at generation buses would be maintained constant while the reactive power output at such buses is within its limits, as in CPF techniques.

B. OPF-DM with Complementarity Constraints

An optimization model that has been empirically shown to yield the same SNB or LISB points as a CPF technique has been proposed in [17]. The authors in this paper propose an optimization model that is based upon the idea that many problems encountered in engineering, physics or economics, which behave according to different rules under different circumstances, can be modeled using complementarity constraints, since these constraints can be used to model a change in system behavior. Thus, the change from a PV to a PQ bus, when a generation reactive power limit is reached, can be modeled using these type of constraints in the OPF problem as follows [31]:

$$\begin{aligned} 0 \leq (Q_{G_k} - Q_{G_{k_{min}}}) \perp V_{a_k} \geq 0 \\ \Rightarrow\ (Q_{G_k} - Q_{G_{k_{min}}}) V_{a_k} = 0 \end{aligned}$$

$$\begin{aligned} 0 \leq (Q_{G_{k_{max}}} - Q_{G_k}) \perp V_{b_k} \geq 0 \\ \Rightarrow\ (Q_{G_k} - Q_{G_{k_{max}}}) V_{b_k} = 0 \end{aligned}$$

where V_a and V_b are auxiliary, nonnegative variables that allow increasing or decreasing the generator voltage set point, depending on the state of Q_G, and $\perp$ is a complementarity operator. Thus:

$$\begin{aligned} \text{if } Q_{G_k} = Q_{G_{k_{min}}} &\Rightarrow V_{a_k} \geq 0 \text{ and } V_{b_k} = 0 \\ \text{if } Q_{G_{k_{min}}} < Q_{G_k} < Q_{G_{k_{max}}} &\Rightarrow V_{a_k} = V_{b_k} = 0 \\ \text{if } Q_{G_k} = Q_{G_{k_{max}}} &\Rightarrow V_{a_k} = 0 \text{ and } V_{b_k} \geq 0 \end{aligned}$$

This yields the following Mixed Complementarity Problem (MCP) [17]:

$$\begin{aligned} \max_{\substack{\delta, V_L, K_G \\ Q_G, V_G, \lambda}} \quad & \lambda \\ \text{s.t.} \quad & G(\delta, V_L, K_G, Q_G, V_G, \lambda, P_S, P_D) = 0 && \text{(15a)} \\ & (Q_{G_k} - Q_{G_{k_{min}}}) V_{a_k} = 0 \quad \forall k \in \mathcal{G} && \text{(15b)} \\ & (Q_{G_k} - Q_{G_{k_{max}}}) V_{b_k} = 0 \quad \forall k \in \mathcal{G} && \text{(15c)} \\ & V_{G_k} = V_{G_{k_o}} + V_{a_k} - V_{b_k} \quad \forall k \in \mathcal{G} && \text{(15d)} \\ & Q_{G_{k_{min}}} \leq Q_{G_k} \leq Q_{G_{k_{max}}} \quad \forall k \in \mathcal{G} && \text{(15e)} \\ & V_{a_k}, V_{b_k} \geq 0 \quad \forall k \in \mathcal{G} && \text{(15f)} \end{aligned}$$

where V_{G_o} is the generator voltage regulator set point, i.e. the generator terminal voltage level if Q_G is within limits; and the constraints (15b)-(15d), associated with the auxiliary variables V_a and V_b, are used to model the actuation limits associated with the generator voltage regulators. Hence, in this model, $\tilde{z} = (\delta, V_L, K_G, V_G)$, $\hat{r} = (Q_G, V_a, V_b)$, $\hat{p} = (P_S, P_D, V_{G_o})$, and $\hat{g}$ and $\hat{h}$ are contained within constraints (15a)-(15d); the actual representation of these two vector functions is discussed in detail in Section V. Observe that generator bus voltage limits are not included in this model, since these limits would basically correspond to "hard" operating limits, as previously discussed with respect to load voltage magnitude limits, generator active power limits, or power transfer limits in (14).

V. Theoretical Analysis of the OPF-DM

In this section, it is formally shown that a solution to the OPF-DM model (15) corresponds to either an SNB or an LISB, by demonstrating that the transversality conditions of the corresponding bifurcations are met, based on the optimality conditions of the optimal solution. Only LIBs associated with maximum reactive power limits are analyzed here, since VS problems in practice are typically associated with generators reaching these limits as the demand in the system increases.

The following assumptions are made for the statement of the theorems and corollary presented next [32]:

- Regularity and strict complementarity conditions must be met at the optimal point, i.e., there must not be degeneracy of the optimization problem at the solution point.
- The solution point must be in a convex region, with the constraints being C^2 and convex at this point.

These assumptions are referred to throughout the rest of the paper as optimality solution (OS) assumptions for convenience. It is important to highlight the fact that there is no guarantee that all possible solutions of (15) would meet these OS assumptions. If these conditions are not met, then the solution could not be classified as an SNB or LIB point with certainty, as per the theorems proved below. However, from numerical results reported in various papers (e.g. [11], [17]), where these types of optimization problems are solved for a variety of small and large electrical power systems, most solutions do meet these assumptions in practice [20]. This is due to the fact that in nonlinear system theory, codimension-1 (single parameter) bifurcations SNBs and LIBs are considered generic [27], i.e. they are expected in power systems under typical operating conditions and modeling assumptions [33].

The theorem below shows that an optimal solution of (15), at which a given generator is at its reactive power limit while its terminal voltage is at its regulator set point, corresponds to an LISB and cannot be an LIDB. This is something one can intuitively deduce from Figure 1(d), if the OS assumptions are met.

Theorem 1: Let $(\hat{z}_c, \lambda_c)$, $\hat{z}_c = (\tilde{z}_c, \hat{r}_c)$, be a local optimum of (15) that meets the aforementioned OS assumptions for $\hat{p} = \hat{p}_o$, where a given generator i satisfies:

$$\left.\begin{array}{c} Q_{G_{i_c}} = Q_{G_{i_{max}}} \\ V_{G_{i_c}} = V_{G_{i_o}} \end{array}\right\} \Rightarrow \quad V_{a_i} = V_{b_i} = 0 \qquad (16)$$

while some other generators $j \neq i \in \mathcal{G}_j \subset \mathcal{G}$ satisfy:

$$\left.\begin{array}{c} Q_{G_{j_c}} = Q_{G_{j_{max}}} \\ V_{G_{j_c}} < V_{G_{j_o}} \end{array}\right\} \Rightarrow \left\{\begin{array}{l} V_{a_j} = 0 \\ V_{b_j} > 0 \end{array}\right. \qquad (17)$$

and the rest of the generators $\bar{j} \neq j \neq i \in \mathcal{G}_{\bar{j}} \subset \mathcal{G}$ are not at their reactive power limits, i.e.

$$\left.\begin{array}{c} Q_{G_{\bar{j}_{min}}} < Q_{G_{\bar{j}_c}} < Q_{G_{\bar{j}_{max}}} \\ V_{G_{\bar{j}_c}} = V_{G_{\bar{j}_o}} \end{array}\right\} \Rightarrow V_{a_{\bar{j}}} = V_{b_{\bar{j}}} = 0 \qquad (18)$$

(Assumptions (17) generalizes the case where an LISB occurs after an LIDB in λ space, as depicted in Fig. 1(d).) Then, $(\hat{z}_c, \lambda_c, \hat{p}_o)$ is an LISB of the power flow model defined by equations (15a)-(15d).

The formal proof to Theorem 1 can be found in Appendix I. This theorem basically proves that a given local optimum of (15) can be an LISB and not an LIDB, and that it can be preceded by some generators reaching reactive power limits, i.e. LIDBs. The following theorem shows that this local optimum can also be an SNB.

Theorem 2: Let $(\hat{z}_c, \lambda_c)$ be local optimum of (15) that meets the abovementioned OS assumptions for $\hat{p} = \hat{p}_o$, where some generators $j \in \mathcal{G}_j \subset \mathcal{G}$ satisfy:

$$\left.\begin{array}{c} Q_{G_{j_c}} = Q_{G_{j_{max}}} \\ V_{G_{j_c}} < V_{G_{j_o}} \end{array}\right\} \Rightarrow \left\{\begin{array}{l} V_{a_j} = 0 \\ V_{b_j} > 0 \end{array}\right. \qquad (19)$$

while the rest of the generators $\bar{j} \neq j \in \mathcal{G}_{\bar{j}} \subset \mathcal{G}$, $\mathcal{G} = \mathcal{G}_{\bar{j}} \cup \mathcal{G}_j$, are not at their reactive power limits, i.e.

$$\left.\begin{array}{c} Q_{G_{\bar{j}_{min}}} < Q_{G_{\bar{j}_c}} < Q_{G_{\bar{j}_{max}}} \\ V_{G_{\bar{j}_c}} = V_{G_{\bar{j}_o}} \end{array}\right\} \Rightarrow V_{a_{\bar{j}}} = V_{b_{\bar{j}}} = 0 \qquad (20)$$

(Assumptions (19) and (20) generalize the case where an SNB occurs after an LIDB in λ space, as depicted in Fig. 1(b).)

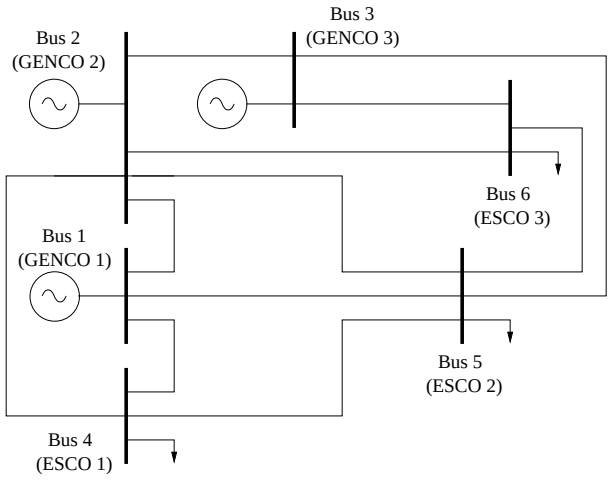

Fig. 2. Six-bus test system.

TABLE I
OPF-DM VS CPF FOR THE 6-BUS TEST SYSTEM

	LISB		SNB (Q limits)		SNB (no Q limits)	
	OPF-DM	CPF	OPF-DM	CPF	OPF-DM	CPF
V_{G_1}	1.0500	1.0500	0.9648	0.9657	1.0500	1.0500
V_{G_2}	1.0025	1.0026	1.0500	1.0500	1.0500	1.0500
V_{G_3}	1.0029	1.0029	1.0500	1.0500	1.0500	1.0500
V_{L_4}	0.8458	0.8458	0.6027	0.6048	0.5360	0.5360
V_{L_5}	0.8546	0.8545	0.8586	0.8591	0.7129	0.7125
V_{L_6}	0.8687	0.8686	0.9465	0.9466	0.7679	0.7677
Q_{G_1}	1.5	1.5	1.5	1.5	3.1588	3.1600
Q_{G_2}	1.5	1.5	0.9577	0.9511	6.2724	6.2734
Q_{G_3}	1.5	1.5	1.4712	1.4682	3.5828	3.5856
λ_c	4.4966	4.5049	1.9046	1.9081	11.1141	11.1330

Then, $(\hat{z}_c, \lambda_c, \hat{p}_o)$ is an SNB of the power flow model defined by equations (15a)-(15d).

The formal proof to Theorem 2 can be found in Appendix II. Finally, the following corollary argues that an optimum of (15) can only be an LISB or an SNB. The proof to this corollary can be found in Appendix III.

Corollary 1: Any solution point $(\hat{z}_c, \lambda_c, \hat{p}_o)$ of (15) that meets the aforementioned OS assumptions is either an LISB or an SNB.

VI. NUMERICAL EXAMPLES

This section presents a numerical comparison between the OPF-DM and the CPF method to illustrate some of the theoretical issues discussed in the previous section. Thus, the maximum loading factor, voltage and reactive power levels obtained from solving (15) are compared with those obtained using the a standard CPF, for a variety of test cases for the 6-bus system shown in Fig. 2 [13], where the generators' voltage set points and reactive power limits are assumed to be $V_{G_o} = 1.05$ p.u. and $Q_G = \pm 1.5$ p.u., respectively.

A. Practical Implementation Issues

The OPF-DM with complementarity constraints can be implemented in AMPL, using the `complements` operator [34], [35], which allows complementarity conditions to be directly specified in the constraint declarations, and then solved using solvers specifically designed for complementarity problems such as KNITRO [36]. Alternatively, the complementarity constraints can be specified as nonsmooth constraints as in (15), solving the optimization problem with nonlinear programming solvers such as LOQO, KNITRO or IPOPT; this is the approach used here to obtain the numerical results discussed in this section. On the other hand, UWPFLOW [37], which is a popular and well-tested software tool with a robust implementation of a CPF technique, was used to obtain PV curves for illustrative and comparison purposes. For both techniques, the generation and load variations were assumed to be defined by (13).

It is important to highlight the fact that the initial operating point is rather important, since it is used to define the generator voltage set points for the optimization problem, as well as the starting point for the CPF, and it must be obtained by running an initial power flow simulation. The auxiliary variables used in the definition of the complementarity constraints must be initialized to zero.

B. Numerical Results

The PV curves in Fig. 3 present three bifurcation profiles under different operating conditions: Fig. 3(a) shows an LISB at $\lambda_c = 4.5049$ p.u., preceded by LIDBs, for the base system topology; Fig. 3(b) shows an SNB at $\lambda_c = 1.9081$ p.u., preceded by LIDBs, when line 2-4 is removed from the system; and Fig. 3(c) shows another SNB at a $\lambda_c = 11.1330$ p.u. when Q-limits are ignored for the base system. Observe in these plots that the bifurcations in the first two cases are preceded by some LIDBs in λ space; also, in the last case, the SNB occurs at a larger loading factor, with the voltages at generator buses remaining constant. Notice as well the sharp "edge" of the bifurcation manifold at the maximum loading point defined by an LISB at λ_c, which is a characteristic of these types of bifurcations, and the "quadratic" shape of the manifolds around the SNBs, which is also typical.

Table I presents a comparison of the solutions obtained using the optimization model (15) as well as the equivalent results obtained from the CPF, as depicted in Fig. 3. The results presented in the first and second columns correspond to the base case, and show that GENCO 1 satisfies the LISB condition $Q_{G_{1_c}} = Q_{G_{1_{max}}}$ and $V_{G_{1_c}} = V_{G_{1_o}}$ at λ_c, while GENCO 2 and GENCO 3 are at their reactive power limits with their voltages below the corresponding set points, i.e. the system has undergone 2 LIDBs before reaching an LISB in λ space, as clearly illustrated in Fig. 3(a). The results in the third and fourth columns, obtained by removing line 2-4, show GENCO 2 and GENCO 3 within their reactive power limits and at their corresponding voltage set points, whereas GENCO 1 has reached its maximum reactive power limit and its voltage is below its set point, indicating the occurrence of an LIDB before the SNB in λ space, as depicted in Fig. 3(b).

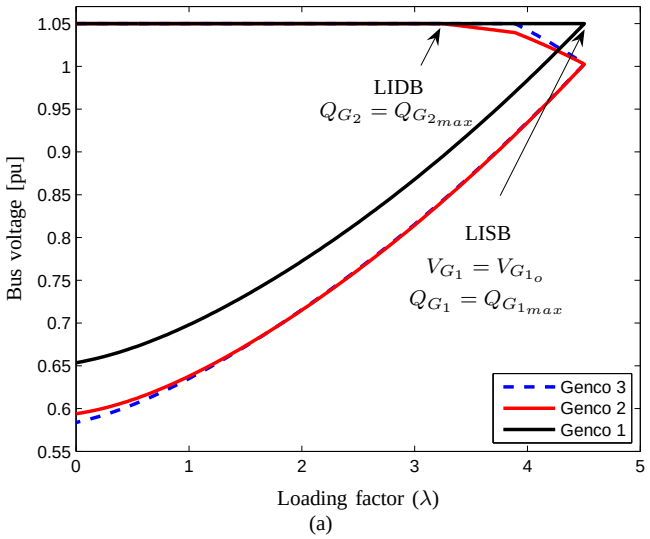

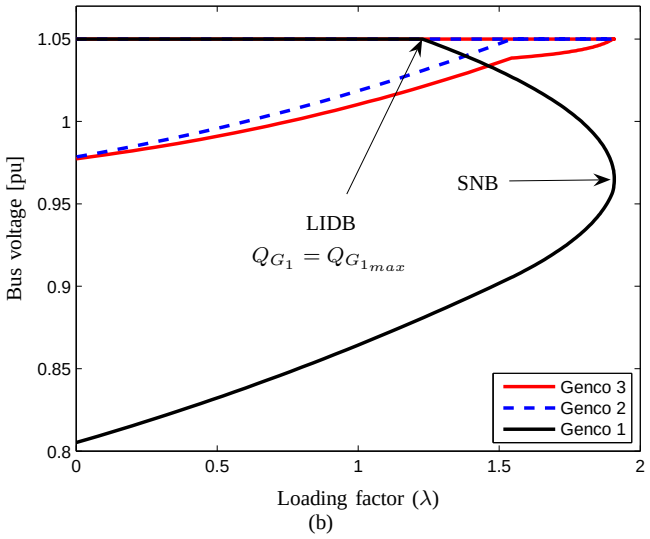

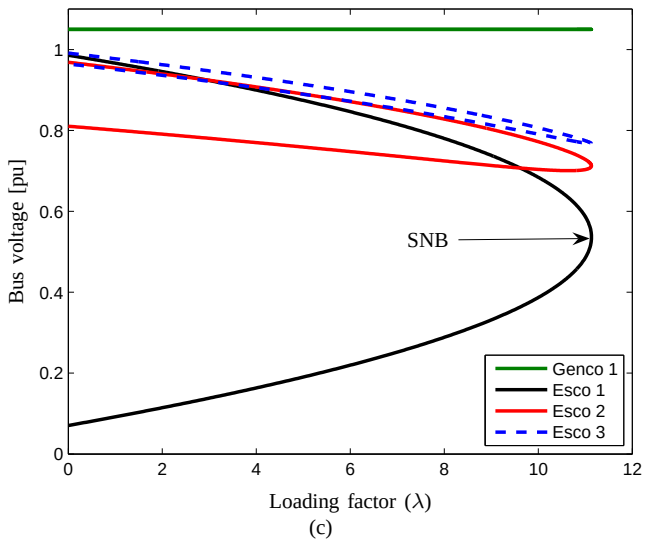

Fig. 3. Generators' PV curves for the 6-bus test system: (a) Base case (LISB preceded by LIDBs); (b) line 2-4 outage (SNB preceded by LIDBs); (c) base system neglecting reactive power limits (SNB).

Finally, the results presented in the last two columns, which correspond to the base system without generator reactive power limits, show all generators at their voltage set points as well as large reactive power outputs, i.e. there are no LIDBs before the SNB in λ space. This table shows that both techniques basically give the same solution; the small differences can be attributed to numerical approximations, particularly in the case of the CPF. The execution time for the OPF-DM was in the range of 0.12 sec, which was faster than the CPF; the reader is referred to [17] for more numerical comparisons in larger systems.

The sequence of generators reaching the maximum reactive power limit can be also obtained from the OPF-DM by calculating the difference $\Delta V_{G_{i_c}} = V_{G_{i_o}} - V_{G_{i_c}}$. Thus, the largest difference corresponds to the first generator reaching its maximum reactive power limit, whereas the smallest one corresponds to last generator. If the difference is negative, then the generator would have reached the minimum reactive power limit. For example, the sorted differences in descending order for the base case are: $\Delta V_{G_{2_c}} = 0.0475$, $\Delta V_{G_{3_c}} = 0.0471$ and $\Delta V_{G_{1_c}} = 0$, which agrees with what is observed in Fig. 3(a).

A test was carried out to study model (14) without complementarity constraints, with the condition that the maximum voltage limit at generation buses is set equal to the voltage set point, i.e. $V_{G_o} = V_{G_{max}}$. This approach can be justified based upon numerical results that show that the voltages at generation buses, if not fixed, typically increase when increasing the load. It is interesting to notice that this possible formulation generated the same results as those obtained from solving (15), shown in Table I. However, this was not the case for other test systems, since such limit $V_{G_{max}}$ does not accurately represent a PV bus, i.e. the constraint $V_{G_o} = V_{G_{max}}$ does not guarantee that V_G is fixed when the reactive power is within limits, which is a condition in (15).

VII. Conclusions

This paper has presented a detailed theoretical study of an optimization method able to determine two types of fold bifurcations directly associated with voltage instabilities in power systems. It was demonstrated that for certain optimality assumptions, which are typically met in practice, the transversality conditions for SNBs and LISBs are met, thus proving that the solution of the studied optimization problem yields the same results as those obtained with the more popular CPF techniques used to analyze these types of bifurcations in power systems.

The advantages of stating the SNB/LIB problem as an optimization problem are that optimization solution techniques can be computational more effective than CPF methods for maximum loadability studies, particularly when using well-tested and efficient solution techniques such as Interior Point Methods. Furthermore, optimization approaches are more versatile than CPF techniques, since the problem can be readily restated so that optimal control parameter values can be calculated to increase the maximum loadability margins of a system.

APPENDIX I
PROOF OF THEOREM 1

Proof: Let $Q_G = (Q_{\overline{G}}, Q_{G_i})$, i.e. the generator reactive power variables are ordered so that generator i is the last variable; similarly for V_G, V_a and V_b. Hence, the Lagrangian function of (15) may then be expressed as:

$$\begin{aligned}\mathcal{L} = \lambda &- \hat{\mu}_1^T G_S(\hat{z}_c, \lambda_c, \hat{p}_o) - \hat{\mu}_2^T G_{Q_{\overline{G}}}(\hat{z}_c, \lambda_c, \hat{p}_o) \\ &- \hat{\mu}_3 G_{Q_{G_i}}(\hat{z}_c, \lambda_c, \hat{p}_o) - \hat{\mu}_4^T (Q_{\overline{G}} - Q_{\overline{G}_{min}}) V_{\bar{a}} \\ &- \hat{\mu}_5^T (Q_{\overline{G}} - Q_{\overline{G}_{max}}) V_{\bar{b}} - \hat{\mu}_6 (Q_{G_i} - Q_{G_{i_{min}}}) V_{a_i} \\ &- \hat{\mu}_7 (Q_{G_i} - Q_{G_{i_{max}}}) V_{b_i} - \hat{\mu}_8^T \left(Q_{\overline{G}_{min}} - Q_{\overline{G}}\right) \\ &- \hat{\mu}_9^T \left(Q_{\overline{G}} - Q_{\overline{G}_{max}}\right) - \hat{\mu}_{10} \left(Q_{G_{i_{min}}} - Q_{G_i}\right) \\ &- \hat{\mu}_{11} \left(Q_{G_i} - Q_{G_{i_{max}}}\right) - \hat{\mu}_{12}^T \left(V_{\overline{G}} - V_{\overline{G}_o} - V_{\bar{a}} + V_{\bar{b}}\right) \\ &- \hat{\mu}_{13} \left(V_{G_i} - V_{G_{i_o}} - V_{a_i} + V_{b_i}\right) - \hat{\mu}_{14}^T (-V_{\bar{a}}) \\ &- \hat{\mu}_{15}^T (-V_{\bar{b}}) - \hat{\mu}_{16} (-V_{a_i}) - \hat{\mu}_{17} (-V_{b_i})\end{aligned}$$

where the functions G_S, $G_{Q_{\overline{G}}}$ and $G_{Q_{G_i}}$ are defined as G in appropriate subsets of variables; and the $\hat{\mu}$s correspond to the Lagrange multipliers of (15).

The KKT optimality conditions state that the gradient of the Lagrangian function must be equal to zero at the optimum [32]. They also state the complementarity condition. Thus:

$$\begin{aligned}
\nabla_\delta \mathcal{L}|_c &= -\nabla_\delta G_S|_c \hat{\mu}_{1_c} - \nabla_\delta G_{Q_{\overline{G}}}|_c \hat{\mu}_{2_c} \\
&\quad -\nabla_\delta G_{Q_{G_i}}|_c \hat{\mu}_{3_c} = 0 && (21)\\
\nabla_{V_L} \mathcal{L}|_c &= -\nabla_{V_L} G_S|_c \hat{\mu}_{1_c} - \nabla_{V_L} G_{Q_{\overline{G}}}|_c \hat{\mu}_{2_c} \\
&\quad -\nabla_{V_L} G_{Q_{G_i}}|_c \hat{\mu}_{3_c} = 0 && (22)\\
\nabla_{K_G} \mathcal{L}|_c &= -\nabla_{K_G} G_S|_c \hat{\mu}_{1_c} = 0 && (23)\\
\nabla_{Q_{\overline{G}}} \mathcal{L}|_c &= -\hat{\mu}_{2_c} - M_{\bar{a}_c} \hat{\mu}_{4_c} - M_{\bar{b}_c} \hat{\mu}_{5_c} + \hat{\mu}_{8_c} - \hat{\mu}_{9_c} = 0 && (24)\\
\nabla_{Q_{G_i}} \mathcal{L}|_c &= -\hat{\mu}_{3_c} - V_{a_{i_c}} \hat{\mu}_{6_c} - V_{b_{i_c}} \hat{\mu}_{7_c} + \hat{\mu}_{10_c} - \hat{\mu}_{11_c} = 0 && (25)\\
\nabla_{V_{\overline{G}}} \mathcal{L}|_c &= -\nabla_{V_{\overline{G}}} G_S|_c \hat{\mu}_{1_c} - \nabla_{V_{\overline{G}}} G_{Q_{\overline{G}}}|_c \hat{\mu}_{2_c} \\
&\quad -\nabla_{V_{\overline{G}}} G_{Q_{G_i}}|_c \hat{\mu}_{3_c} - \hat{\mu}_{12_c} = 0 && (26)\\
\nabla_{V_{G_i}} \mathcal{L}|_c &= -\nabla_{V_{G_i}} G_S|_c \hat{\mu}_{1_c} - \nabla_{V_{G_i}} G_{Q_{\overline{G}}}|_c \hat{\mu}_{2_c} \\
&\quad -\nabla_{V_{G_i}} G_{Q_{G_i}}|_c \hat{\mu}_{3_c} - \hat{\mu}_{13_c} = 0 && (27)\\
\nabla_\lambda \mathcal{L}|_c &= -\nabla_\lambda G_S|_c \hat{\mu}_{1_c} - \nabla_\lambda G_{Q_{\overline{G}}}|_c \hat{\mu}_{2_c} \\
&\quad -\nabla_\lambda G_{Q_{G_i}}|_c \hat{\mu}_{3_c} + 1 = 0 && (28)\\
\nabla_{V_{\bar{a}}} \mathcal{L}|_c &= -M_{Q_{\overline{G}_{min_c}}} \hat{\mu}_{4_c} + \hat{\mu}_{12_c} + \hat{\mu}_{14_c} = 0 && (29)\\
\nabla_{V_{\bar{b}}} \mathcal{L}|_c &= -M_{Q_{\overline{G}_{max_c}}} \hat{\mu}_{5_c} - \hat{\mu}_{12_c} + \hat{\mu}_{15_c} = 0 && (30)\\
\nabla_{V_{a_i}} \mathcal{L}|_c &= -(Q_{G_{i_c}} - Q_{G_{i_{min}}}) \hat{\mu}_{6_c} + \hat{\mu}_{13_c} + \hat{\mu}_{16_c} = 0 && (31)\\
\nabla_{V_{b_i}} \mathcal{L}|_c &= -(Q_{G_{i_c}} - Q_{G_{i_{max}}}) \hat{\mu}_{7_c} - \hat{\mu}_{13_c} + \hat{\mu}_{17_c} = 0 && (32)
\end{aligned}$$

where $M_{\bar{a}_c} = \text{diag}(V_{\bar{a}_c})$, $M_{\bar{b}_c} = \text{diag}(V_{\bar{b}_c})$, $M_{Q_{\overline{G}_{min_c}}} = \text{diag}(Q_{\overline{G}_c} - Q_{\overline{G}_{min}})$, and $M_{Q_{\overline{G}_{max_c}}} = \text{diag}(Q_{\overline{G}_c} - Q_{\overline{G}_{max}})$ are diagonal matrices. Also, the equality constraints must be equal to zero and the inequality constraints are less than or equal to zero at the optimum, i.e. this point must be feasible.

The complementarity slackness condition provides an indication of whether an inequality constraint is active or not. Hence, based on the regularity and strict complementarity OS assumptions, which imply that $\mu_c = (\mu_{1_c}, \ldots, \mu_{17_c}) \neq 0$ is unique, and $\mu_{l_c} > 0 \ \forall l \in \{\text{Active Constraint Set}\}$ [32], it follows from (16)-(18) that:

$$\begin{aligned}
\hat{\mu}_{8_{k_c}} (Q_{G_{k_{min}}} - Q_{G_{k_c}}) = 0 \ &\Rightarrow \ \hat{\mu}_{8_{k_c}} = 0 \ \forall k \in \bar{\mathcal{G}} && (33)\\
\hat{\mu}_{9_{\bar{j}_c}} (Q_{G_{\bar{j}_c}} - Q_{G_{\bar{j}max}}) = 0 \ &\Rightarrow \ \hat{\mu}_{9_{\bar{j}_c}} = 0 \ \forall \bar{j} \in \mathcal{G}_{\bar{j}} && (34)\\
\hat{\mu}_{9_{j_c}} (Q_{G_{j_c}} - Q_{G_{jmax}}) = 0 \ &\Rightarrow \ \hat{\mu}_{9_{j_c}} > 0 \ \forall j \in \mathcal{G}_j && (35)\\
\hat{\mu}_{10_c} (Q_{G_{i_{min}}} - Q_{G_{i_c}}) = 0 \ &\Rightarrow \ \hat{\mu}_{10_c} = 0 && (36)\\
\hat{\mu}_{11_c} (Q_{G_{i_c}} - Q_{G_{i_{max}}}) = 0 \ &\Rightarrow \ \hat{\mu}_{11_c} > 0 && (37)\\
\hat{\mu}_{14_{k_c}} (-V_{a_{k_c}}) = 0 \ &\Rightarrow \ \hat{\mu}_{14_{k_c}} > 0 \ \forall k \in \bar{\mathcal{G}} && (38)\\
\hat{\mu}_{15_{\bar{j}_c}} (-V_{b_{\bar{j}_c}}) = 0 \ &\Rightarrow \ \hat{\mu}_{15_{\bar{j}_c}} > 0 \ \forall \bar{j} \in \mathcal{G}_{\bar{j}} && (39)\\
\hat{\mu}_{15_{j_c}} (-V_{b_{j_c}}) = 0 \ &\Rightarrow \ \hat{\mu}_{15_{j_c}} = 0 \ \forall j \in \mathcal{G}_j && (40)\\
\hat{\mu}_{16_c} (-V_{a_{i_c}}) = 0 \ &\Rightarrow \ \hat{\mu}_{16_c} > 0 && (41)\\
\hat{\mu}_{17_c} (-V_{b_{i_c}}) = 0 \ &\Rightarrow \ \hat{\mu}_{17_c} > 0 && (42)
\end{aligned}$$

where $\bar{\mathcal{G}} = \mathcal{G}_{\bar{j}} \cup \mathcal{G}_j$.

Now, based on (16)-(18), the following actuation regime and saturation regime equations, evaluated at the solution point $(\hat{z}_c, \lambda_c, \hat{p}_o)$, are the minimum subsets of constraints (15a)-(15f) that uniquely define $\hat{z}_c$ for a given $(\lambda_c, \hat{p}_o)$, since the number of equations and unknowns is the same, i.e. $N = 2n_b + n_{\mathcal{G}}$, where n_b is the number of system buses and $n_{\mathcal{G}}$ is the number of generators:

$$G_a|_c = \begin{bmatrix} G(\delta_c, V_{L_c}, K_{G_c}, Q_{G_c}, V_{G_c}, \lambda_c, P_{S_o}, P_{D_o}) \\ V_{G_{\bar{j}_c}} - V_{G_{\bar{j}_o}} \quad \forall \bar{j} \in \mathcal{G}_{\bar{j}} \\ Q_{G_{j_c}} - Q_{G_{j_{max}}} \quad \forall j \in \mathcal{G}_j \\ V_{G_{i_c}} - V_{G_{i_o}} \end{bmatrix} = 0 \quad (43)$$

$$G_b|_c = \begin{bmatrix} G(\delta_c, V_{L_c}, K_{G_c}, Q_{G_c}, V_{G_c}, \lambda_c, P_{S_o}, P_{D_o}) \\ V_{G_{\bar{j}_c}} - V_{G_{\bar{j}_o}} \quad \forall \bar{j} \in \mathcal{G}_{\bar{j}} \\ Q_{G_{j_c}} - Q_{G_{j_{max}}} \quad \forall j \in \mathcal{G}_j \\ Q_{G_{i_c}} - Q_{G_{i_{max}}} \end{bmatrix} = 0 \quad (44)$$

Notice that these equations have a similar form as (8) and (9), respectively, where $\tilde{z}_c = (\delta_c, V_{L_c}, K_{G_c}, V_{G_c})$, $\hat{r}_c = Q_{G_c}$, $\hat{p}_o = (P_{S_o}, P_{D_o}, V_{G_o})$, $\hat{g}|_c = G|_c$, and

$$\hat{r}_c - \hat{s}|_c \equiv \begin{bmatrix} V_{G_{\bar{j}_c}} - V_{G_{\bar{j}_o}} \quad \forall \bar{j} \in \mathcal{G}_{\bar{j}} \\ Q_{G_{j_c}} - Q_{G_{j_{max}}} \quad \forall j \in \mathcal{G}_j \\ V_{G_{i_c}} - V_{G_{i_o}} \end{bmatrix}$$

Observe that in this case, some of the actuation limit functions are implicit instead of explicit functions of the corresponding variables $\hat{r}$. Hence, for the optimal solution to be an LISB, one first must prove that the Jacobians J_a^i and J_b^i associated with (43) and (44) are nonsingular.

Let first prove that J_b^i is not singular. Hence, from (21)-(32) and with the proper ordering of variables and equations in (44), and assuming that $V_{\overline{G}} = (V_{G_{\bar{j}}} \ \forall \bar{j} \in \mathcal{G}_{\bar{j}}, V_{G_j} \ \forall j \in \mathcal{G}_j)$, and similarly for $Q_{\overline{G}}$, it can be shown that:

$$J_b^{i^T} \hat{x}_b = \hat{b}_b \quad (45)$$

where

$$J_b^{i^T} = \left[\begin{array}{ccccc|c} \nabla_\delta G_S|_c & \nabla_\delta G_{Q_{\overline{G}}}|_c & \nabla_\delta G_{Q_{G_i}}|_c & 0 & 0 & 0 \\ \nabla_{V_L} G_S|_c & \nabla_{V_L} G_{Q_{\overline{G}}}|_c & \nabla_{V_L} G_{Q_{G_i}}|_c & 0 & 0 & 0 \\ \nabla_{K_G} G_S|_c & 0 & 0 & 0 & 0 & 0 \\ \nabla_{V_{\overline{G}}} G_S|_c & \nabla_{V_{\overline{G}}} G_{Q_{\overline{G}}}|_c & \nabla_{V_{\overline{G}}} G_{Q_{G_i}}|_c & U & 0 & 0 \\ 0 & I_{n_{\bar{\mathcal{G}}}} & 0 & 0 & W & 0 \\ 0 & 0 & 1 & 0 & 0 & 1 \\ \hline \nabla_{V_{G_i}} G_S|_c & \nabla_{V_{G_i}} G_{Q_{\overline{G}}}|_c & \nabla_{V_{G_i}} G_{Q_{G_i}}|_c & 0 & 0 & 0 \end{array}\right] \quad (46)$$

$$= \left[\begin{array}{c|c} A^T & e \\ \hline c^T & 0 \end{array}\right]$$

$$\hat{x}_b = \left[\begin{array}{c} \hat{\mu}_{1_c} \\ \hat{\mu}_{2_c} \\ \hat{\mu}_{3_c} \\ \hat{\mu}_{12_{\mathcal{G}_{\bar{j}_c}}} \\ \hat{\mu}_{9_{\mathcal{G}_{j_c}}} \\ \hline \hat{\mu}_{11_c} \end{array}\right]$$

$$\hat{b}_b = \left[\begin{array}{c} 0 \\ 0 \\ 0 \\ -W\hat{\mu}_{12_{\mathcal{G}_{j_c}}} \\ -M_{\bar{a}_c}\hat{\mu}_{4_c} - M_{\bar{b}_c}\hat{\mu}_{5_c} + \hat{\mu}_{8_c} - U\hat{\mu}_{9_{\mathcal{G}_{\bar{j}_c}}} \\ \hline -V_{a_{i_c}}\hat{\mu}_{6_c} - V_{b_{i_c}}\hat{\mu}_{7_c} + \hat{\mu}_{10_c} \\ \hline \hat{\mu}_{13_c} \end{array}\right]$$

and $\hat{\mu}_9 = (\hat{\mu}_{9_{\mathcal{G}_{\bar{j}}}}, \hat{\mu}_{9_{\mathcal{G}_j}})$, $\hat{\mu}_{12} = (\hat{\mu}_{12_{\mathcal{G}_{\bar{j}}}}, \hat{\mu}_{12_{\mathcal{G}_j}})$,

$$U = \left[\begin{array}{c} I_{n_{\mathcal{G}_{\bar{j}}}} \\ 0 \end{array}\right], \quad W = \left[\begin{array}{c} 0 \\ I_{n_{\mathcal{G}_j}} \end{array}\right]$$

where I_n is an $n \times n$ identity matrix.

Now, from (25), (36) and (37):

$$\hat{\mu}_{3_c} = -\hat{\mu}_{11_c} \neq 0 \quad (47)$$

From (35)

$$\hat{\mu}_{9_{\mathcal{G}_{j_c}}} \neq 0 \quad (48)$$

And from (32) and (42)

$$\hat{\mu}_{13_c} = \hat{\mu}_{17_c} \neq 0 \quad (49)$$

Hence, from (47)-(49), it follows that:

$$\hat{x}_b \neq 0 \quad \text{and} \quad \hat{b}_b \neq 0$$

and are both unique. Therefore, one can conclude from (45) that J_b^i is nonsingular, i.e.

$$\det(J_b^i) \neq 0 \quad (50)$$

With similar arguments, it can be readily shown that:

$$J_a^{i^T}\hat{x}_a = \hat{b}_a \quad (51)$$

where

$$J_a^{i^T} = \left[\begin{array}{c|c} A^T & 0 \\ \hline c^T & 1 \end{array}\right] \quad (52)$$

$$\hat{x}_a = \left[\begin{array}{c} \hat{\mu}_{1_c} \\ \hat{\mu}_{2_c} \\ \hat{\mu}_{3_c} \\ \hat{\mu}_{12_{\mathcal{G}_{\bar{j}_c}}} \\ \hat{\mu}_{9_{\mathcal{G}_{j_c}}} \\ \hline \hat{\mu}_{13_c} \end{array}\right]$$

$$\hat{b}_a = \left[\begin{array}{c} 0 \\ 0 \\ 0 \\ -W\hat{\mu}_{12_{\mathcal{G}_{j_c}}} \\ -M_{\bar{a}_c}\hat{\mu}_{4_c} - M_{\bar{b}_c}\hat{\mu}_{5_c} + \hat{\mu}_{8_c} - U\hat{\mu}_{9_{\mathcal{G}_{\bar{j}_c}}} \\ \hline -V_{a_{i_c}}\hat{\mu}_{6_c} - V_{b_{i_c}}\hat{\mu}_{7_c} + \hat{\mu}_{10_c} - \hat{\mu}_{11_c} \\ \hline 0 \end{array}\right]$$

Therefore, from (47)-(49), it follows that:

$$\hat{x}_a \neq 0 \quad \text{and} \quad \hat{b}_a \neq 0$$

and are both unique, yielding from (51) a nonsingular J_a^i, i.e.

$$\det(J_a^i) \neq 0 \quad (53)$$

Thus, from (50) and (53), it is clear that the solution point $(\hat{z}_c, \lambda_c, \hat{p}_o)$ meets transversality conditions (10).

The second transversality condition (11) simply states that the ratio of the determinants of J_a^i and J_b^i must be positive for $(\hat{z}_c, \lambda_c, \hat{p}_o)$ to be an LISB. Thus, from (46) and (52), and based on Schur's Complements [38], it follows that:

$$\begin{aligned} \det(J_a^i) &= \det(A) \\ \det(J_b^i) &= -e^T A^{-1} c \det(A) \end{aligned}$$

Therefore:

$$\alpha = \frac{\det(J_a^i)}{\det(J_b^i)} = \frac{1}{-e^T A^{-1} c} \quad (54)$$

Then, from (43), it follows that:

$$\nabla_{\hat{z}}^T G_a|_c \, \mathrm{d}\hat{z} + \nabla_{V_{G_{i_o}}}^T G_a|_c \, \mathrm{d}V_{G_{i_o}} = 0$$

which from (52) can be rewritten as:

$$\left[\begin{array}{c|c} A & c \\ \hline 0 & 1 \end{array}\right] \left[\begin{array}{c} \mathrm{d}\bar{z} \\ \hline \mathrm{d}V_{G_i} \end{array}\right] - \left[\begin{array}{c} 0 \\ \hline 1 \end{array}\right] \mathrm{d}V_{G_{i_o}} = 0$$

where $\hat{z} = (\bar{z}, V_{G_i})$. This yields:

$$\mathrm{d}\bar{z} = -A^{-1} c \, \mathrm{d}V_{G_i} \quad (55)$$

$$\mathrm{d}V_{G_i} = \mathrm{d}V_{G_{i_o}} \quad (56)$$

On the other hand, from (44) and (46), one has that:

$$\left[\begin{array}{c|c} A & c \\ \hline e^T & 0 \end{array}\right] \left[\begin{array}{c} \mathrm{d}\bar{z} \\ \hline \mathrm{d}V_{G_i} \end{array}\right] - \left[\begin{array}{c} 0 \\ \hline 1 \end{array}\right] \mathrm{d}Q_{G_{i_{max}}} = 0$$

which yields (55) as well as:

$$\mathrm{d}Q_{G_i} = e^T \, \mathrm{d}\bar{z} = \mathrm{d}Q_{G_{i_{max}}} \quad (57)$$

Thus, from (55), (56) and (57), it follows that:

$$\left.\frac{\mathrm{d}Q_{G_{i_{max}}}}{\mathrm{d}V_{G_{i_o}}}\right|_c = -e^T A^{-1} c$$

which, from (54), leads to:

$$\alpha = \left.\frac{\mathrm{d}V_{G_{i_o}}}{\mathrm{d}Q_{G_{i_{max}}}}\right|_c \tag{58}$$

Now, from the optimization model (15), the sensitivities of the objective function with respect to $Q_{G_{i_{max}}}$ and and $V_{G_{i_o}}$ evaluated at the optimal point can be stated as [39]:

$$\begin{aligned}\hat{\mu}_{11_c} &= \left.\frac{d\lambda}{dQ_{G_{i_{max}}}}\right|_c \\ \hat{\mu}_{13_c} &= \left.\frac{d\lambda}{dV_{G_{i_o}}}\right|_c\end{aligned}$$

Hence, from (37), (49), and (58), it follows that:

$$\alpha = \frac{\hat{\mu}_{11_c}}{\hat{\mu}_{13_c}} > 0 \tag{59}$$

which satisfies the second transversality condition (11). Therefore, the optimal solution $(\hat{z}_c, \lambda_c, \hat{p}_o)$ which meets the given OS assumptions is an LISB.

Finally, observe that, at an LIDB, assumptions (16)-(18) are also met. However, (59) rules out the possibility of an LIDB being a solution of (15). ■

APPENDIX II
PROOF OF THEOREM 2

Proof: Following a similar approach to the proof of Theorem 1, let $Q_G = (Q_{\overline{G}}, Q_{\widetilde{G}})$, where $Q_{\overline{G}} = (Q_{G_{\bar{j}}}\ \forall \bar{j} \in \mathcal{G}_{\bar{j}}, Q_{G_j}\ \forall j \in \mathcal{G}_j)$, and similarly for V_G, V_a and V_b. Hence, the Lagrangian function of (15) may then be expressed as:

$$\begin{aligned}\mathcal{L} = \lambda &- \hat{\mu}_1^T G_S(\hat{z}_c, \lambda_c, \hat{p}_o) - \hat{\mu}_2^T G_{Q_{\overline{G}}}(\hat{z}_c, \lambda_c, \hat{p}_o) \\ &- \hat{\mu}_3 G_{Q_{\widetilde{G}}}(\hat{z}_c, \lambda_c, \hat{p}_o) - \hat{\mu}_4^T (Q_{\overline{G}} - Q_{\overline{G}_{min}}) V_{\bar{a}} \\ &- \hat{\mu}_5^T (Q_{\overline{G}} - Q_{\overline{G}_{max}}) V_{\bar{b}} - \hat{\mu}_6^T (Q_{\widetilde{G}} - Q_{\widetilde{G}_{min}}) V_{\tilde{a}} \\ &- \hat{\mu}_7^T (Q_{\widetilde{G}} - Q_{\widetilde{G}_{max}}) V_{\tilde{b}} - \hat{\mu}_8^T \left(Q_{\overline{G}_{min}} - Q_{\overline{G}}\right) \\ &- \hat{\mu}_9^T \left(Q_{\overline{G}} - Q_{\overline{G}_{max}}\right) - \hat{\mu}_{10}^T \left(Q_{\widetilde{G}_{min}} - Q_{\widetilde{G}}\right) \\ &- \hat{\mu}_{11}^T \left(Q_{\widetilde{G}} - Q_{\widetilde{G}_{max}}\right) - \hat{\mu}_{12}^T \left(V_{\overline{G}} - V_{\overline{G}_o} - V_{\bar{a}} + V_{\bar{b}}\right) \\ &- \hat{\mu}_{13} \left(V_{\widetilde{G}} - V_{\widetilde{G}_o} - V_{\tilde{a}} + V_{\tilde{b}}\right) - \hat{\mu}_{14}^T (-V_{\bar{a}}) \\ &- \hat{\mu}_{15}^T (-V_{\bar{b}}) - \hat{\mu}_{16}^T (-V_{\tilde{a}}) - \hat{\mu}_{17}^T (-V_{\tilde{b}})\end{aligned}$$

From the KKT optimality conditions, it follows that:

$$\begin{aligned}\nabla_\delta \mathcal{L}|_c &= -\nabla_\delta G_S|_c \hat{\mu}_{1_c} - \nabla_\delta G_{Q_{\overline{G}}}|_c \hat{\mu}_{2_c} \\ &\quad -\nabla_\delta G_{Q_{\widetilde{G}}}|_c \hat{\mu}_{3_c} = 0 \qquad (60)\\ \nabla_{V_L} \mathcal{L}|_c &= -\nabla_{V_L} G_S|_c \hat{\mu}_{1_c} - \nabla_{V_L} G_{Q_{\overline{G}}}|_c \hat{\mu}_{2_c} \\ &\quad -\nabla_{V_L} G_{Q_{\widetilde{G}}}|_c \hat{\mu}_{3_c} = 0 \qquad (61)\\ \nabla_{K_G} \mathcal{L}|_c &= -\nabla_{K_G} G_S|_c \hat{\mu}_{1_c} = 0 \qquad (62)\\ \nabla_{Q_{\overline{G}}} \mathcal{L}|_c &= -\hat{\mu}_{2_c} - M_{\bar{a}_c} \hat{\mu}_{4_c} - M_{\bar{b}_c} \hat{\mu}_{5_c} + \hat{\mu}_{8_c} - \hat{\mu}_{9_c} = 0 \qquad (63)\\ \nabla_{Q_{\widetilde{G}}} \mathcal{L}|_c &= -\hat{\mu}_{3_c} - M_{\tilde{a}_c} \hat{\mu}_{6_c} - M_{\tilde{b}_c} \hat{\mu}_{7_c} + \hat{\mu}_{10_c} - \hat{\mu}_{11_c} = 0 \qquad (64)\\ \nabla_{V_{\overline{G}}} \mathcal{L}|_c &= -\nabla_{V_{\overline{G}}} G_S|_c \hat{\mu}_{1_c} - \nabla_{V_{\overline{G}}} G_{Q_{\overline{G}}}|_c \hat{\mu}_{2_c} \\ &\quad -\nabla_{V_{\overline{G}}} G_{Q_{\widetilde{G}}}|_c \hat{\mu}_{3_c} - \hat{\mu}_{12_c} = 0 \qquad (65)\\ \nabla_{V_{\widetilde{G}}} \mathcal{L}|_c &= -\nabla_{V_{\widetilde{G}}} G_S|_c \hat{\mu}_{1_c} - \nabla_{V_{\widetilde{G}}} G_{Q_{\overline{G}}}|_c \hat{\mu}_{2_c} \\ &\quad -\nabla_{V_{\widetilde{G}}} G_{Q_{\widetilde{G}}}|_c \hat{\mu}_{3_c} - \hat{\mu}_{13_c} = 0 \qquad (66)\\ \nabla_\lambda \mathcal{L}|_c &= -\nabla_\lambda G_S|_c \hat{\mu}_{1_c} - \nabla_\lambda G_{Q_{\overline{G}}}|_c \hat{\mu}_{2_c} \\ &\quad -\nabla_\lambda G_{Q_{\widetilde{G}}}|_c \hat{\mu}_{3_c} + 1 = 0 \qquad (67)\end{aligned}$$

$$\begin{aligned}\nabla_{V_{\bar{a}}} \mathcal{L}|_c &= -M_{Q_{\overline{G}_{min_c}}} \hat{\mu}_{4_c} + \hat{\mu}_{12_c} + \hat{\mu}_{14_c} = 0 \qquad (68)\\ \nabla_{V_{\bar{b}}} \mathcal{L}|_c &= -M_{Q_{\overline{G}_{max_c}}} \hat{\mu}_{5_c} - \hat{\mu}_{12_c} + \hat{\mu}_{15_c} = 0 \qquad (69)\\ \nabla_{V_{\tilde{a}}} \mathcal{L}|_c &= -M_{Q_{\widetilde{G}_{min_c}}} \hat{\mu}_{6_c} + \hat{\mu}_{13_c} + \hat{\mu}_{16_c} = 0 \qquad (70)\\ \nabla_{V_{\tilde{b}}} \mathcal{L}|_c &= -M_{Q_{\widetilde{G}_{max_c}}} \hat{\mu}_{7_c} - \hat{\mu}_{13_c} + \hat{\mu}_{17_c} = 0 \qquad (71)\end{aligned}$$

where $M_{\bar{a}_c} = \mathrm{diag}(V_{\bar{a}_c})$, and similarly for $M_{\bar{b}_c}$, $M_{\tilde{a}_c}$, $M_{\tilde{b}_c}$; and $M_{Q_{\overline{G}_{min_c}}} = \mathrm{diag}(Q_{\overline{G}_c} - Q_{\overline{G}_{min}})$, and similarly for $M_{Q_{\overline{G}_{max_c}}}$, $M_{Q_{\widetilde{G}_{min_c}}}$, and $M_{Q_{\widetilde{G}_{max_c}}}$. Furthermore, all the equality constraints must be equal to zero, while the inequality constraints must be less than or equal to zero.

From the regularity and strict complementarity OS assumptions, which imply a unique $\mu_c = (\mu_{1_c}, \ldots, \mu_{17_c}) \neq 0$, with $\mu_{l_c} > 0\ \forall l \in \{\text{Active Constraint Set}\}$, it follows from (19) and (20) that:

$$\begin{aligned}\hat{\mu}_{8_{\bar{j}_c}} (Q_{G_{\bar{j}_{min}}} - Q_{G_{\bar{j}_c}}) = 0 \ &\Rightarrow\ \hat{\mu}_{8_{\bar{j}_c}} = 0\ \forall \bar{j} \in \mathcal{G}_{\bar{j}} \qquad (72)\\ \hat{\mu}_{9_{\bar{j}_c}} (Q_{G_{\bar{j}_c}} - Q_{G_{\bar{j}_{max}}}) = 0 \ &\Rightarrow\ \hat{\mu}_{9_{\bar{j}_c}} = 0\ \forall \bar{j} \in \mathcal{G}_{\bar{j}} \qquad (73)\\ \hat{\mu}_{10_{j_c}} (Q_{G_{j_{min}}} - Q_{G_{j_c}}) = 0 \ &\Rightarrow\ \hat{\mu}_{10_{j_c}} = 0\ \forall j \in \mathcal{G}_j \qquad (74)\\ \hat{\mu}_{11_{j_c}} (Q_{G_{j_c}} - Q_{G_{j_{max}}}) = 0 \ &\Rightarrow\ \hat{\mu}_{11_{j_c}} > 0\ \forall j \in \mathcal{G}_j \qquad (75)\\ \hat{\mu}_{14_{\bar{j}_c}} (-V_{a_{\bar{j}_c}}) = 0 \ &\Rightarrow\ \hat{\mu}_{14_{\bar{j}_c}} > 0\ \forall \bar{j} \in \mathcal{G}_{\bar{j}} \qquad (76)\\ \hat{\mu}_{15_{\bar{j}_c}} (-V_{b_{\bar{j}_c}}) = 0 \ &\Rightarrow\ \hat{\mu}_{15_{\bar{j}_c}} > 0\ \forall \bar{j} \in \mathcal{G}_{\bar{j}} \qquad (77)\\ \hat{\mu}_{16_{j_c}} (-V_{a_{j_c}}) = 0 \ &\Rightarrow\ \hat{\mu}_{16_{j_c}} > 0\ \forall j \in \mathcal{G}_j \qquad (78)\\ \hat{\mu}_{17_{j_c}} (-V_{b_{j_c}}) = 0 \ &\Rightarrow\ \hat{\mu}_{17_{j_c}} = 0\ \forall j \in \mathcal{G}_j \qquad (79)\end{aligned}$$

Now, based on (19) and (20), the following equations, evaluated at the solution point $(\hat{z}_c, \lambda_c, \hat{p}_o)$, form the minimum subset of constraints (15a)-(15f) that uniquely define $\hat{z}_c$ for a given $(\lambda_c, \hat{p}_o)$, since the number of equations and unknowns is the same, i.e. N:

$$G|_c = \begin{bmatrix} G(\delta_c, V_{L_c}, K_{G_c}, Q_{G_c}, V_{G_c}, \lambda_c, P_{S_o}, P_{D_o}) \\ V_{\overline{G}_c} - V_{\overline{G}_o} \\ Q_{\widetilde{G}_c} - Q_{\widetilde{G}_{max}} \end{bmatrix} = 0 \tag{80}$$

Hence, for the optimal solution to be an SNB, one first must prove that the Jacobian $J = \nabla_{\hat{z}}^T G|_c$ is singular with unique nonzero eigenvectors, where $\hat{z} = (\delta, V_L, K_G, V_G, Q_G)$.

From (60)-(71) and with the proper ordering of variables and equations in (44), it can be shown that:

$$\nabla_{\hat{z}} G|_c\ \hat{w} = \hat{b} \tag{81}$$

where,

$$\nabla_{\hat{z}} G|_c = \tag{82}$$

$$\begin{bmatrix} \nabla_\delta G_S|_c & \nabla_\delta G_{Q_{\overline{G}}}|_c & \nabla_\delta G_{Q_{\widetilde{G}}}|_c & 0 & 0 \\ \nabla_{V_L} G_S|_c & \nabla_{V_L} G_{Q_{\overline{G}}}|_c & \nabla_{V_L} G_{Q_{\widetilde{G}}}|_c & 0 & 0 \\ \nabla_{K_G} G_S|_c & 0 & 0 & 0 & 0 \\ \nabla_{V_{\overline{G}}} G_S|_c & \nabla_{V_{\overline{G}}} G_{Q_{\overline{G}}}|_c & \nabla_{V_{\overline{G}}} G_{Q_{\widetilde{G}}}|_c & I_{n_{\mathcal{G}_{\bar{j}}}} & 0 \\ \nabla_{V_{\widetilde{G}}} G_S|_c & \nabla_{V_{\widetilde{G}}} G_{Q_{\overline{G}}}|_c & \nabla_{V_{\widetilde{G}}} G_{Q_{\widetilde{G}}}|_c & 0 & 0 \\ 0 & I_{n_{\mathcal{G}_{\bar{j}}}} & 0 & 0 & 0 \\ 0 & 0 & I_{n_{\mathcal{G}_j}} & 0 & I_{n_{\mathcal{G}_j}} \end{bmatrix}$$

$$\hat{w} = \begin{bmatrix} \hat{\mu}_{1_c} \\ \hat{\mu}_{2_c} \\ \hat{\mu}_{3_c} \\ \hat{\mu}_{12_c} \\ \hat{\mu}_{11_c} + M_{\tilde{b}_c}\hat{\mu}_{7_c} \end{bmatrix} \tag{83}$$

$$\hat{b} = \begin{bmatrix} 0 \\ 0 \\ 0 \\ 0 \\ -\hat{\mu}_{13_c} \\ -M_{\bar{a}_c}\hat{\mu}_{4_c} - M_{\bar{b}_c}\hat{\mu}_{5_c} + \hat{\mu}_{8_c} - \hat{\mu}_{9_c} \\ -M_{\tilde{a}_c}\hat{\mu}_{6_c} + \hat{\mu}_{10_c} \end{bmatrix}$$

Now, from (71) and (79):

$$\hat{\mu}_{13_c} = \hat{\mu}_{17_c} = 0 \tag{84}$$

From (20), (72) and (73):

$$-M_{\bar{a}_c}\hat{\mu}_{4_c} - M_{\bar{b}_c}\hat{\mu}_{5_c} + \hat{\mu}_{8_c} - \hat{\mu}_{9_c} = 0 \tag{85}$$

From (19) and (74):

$$-M_{\tilde{a}_c}\hat{\mu}_{6_c} + \hat{\mu}_{10_c} = 0 \tag{86}$$

Hence, from (84)-(86), it follows that:

$$\nabla_{\hat{z}} G|_c \, \hat{w} = 0$$

Finally, since, from the regularity and strict complementarity OS assumptions, it follows that $\mu_{1_c} \neq 0$, $\mu_{2_c} \neq 0$, and $\mu_{3_c} \neq 0$, as $\hat{\mu}_c \neq 0$ and is unique. Hence, $\hat{w} \neq 0$ and is unique, from which it can be concluded that the optimum $(\hat{z}_c, \lambda_c, \hat{p}_o)$ meets the SNB transversality condition (3).

Now, from (67), (80) and (83), it follows that:

$$\nabla_{\lambda} \mathcal{L}|_c = -\nabla_{\lambda} G|_c \, \hat{w} + 1 = 0$$

$$\Rightarrow \; \nabla_{\lambda} G|_c \, \hat{w} \neq 0$$

which corresponds to the SNB transversality condition (4).

The third SNB transversality condition (5) is now verified. Thus, from assumptions (19) and (20) regarding the optimum $(\hat{z}_c, \lambda_c, \hat{p}_o)$, and from (80), as well as based on the previous analysis, the optimization model (15) can be restated as follows, since it would yield the same optimal solution:

$$\begin{aligned} \max \quad & \lambda \\ \text{s.t.} \quad & G(\hat{z}, \lambda, \hat{p}_o) = 0 \end{aligned}$$

The corresponding Lagrangian function may then be defined as:

$$\mathcal{L}(\hat{z}, \lambda, \hat{p}_o, \hat{\mu}) = \lambda - \hat{\mu}^T G(\hat{z}, \lambda, \hat{p}_o)$$

which, based on the KKT optimality conditions, leads to:

$$\nabla_{\hat{z}} \mathcal{L}|_c = -\nabla_{\hat{z}} G|_c \hat{\mu}_c = -\nabla_{\hat{z}} G|_c \hat{w} = 0 \tag{88}$$

$$\nabla_{\hat{\mu}} \mathcal{L}|_c = -G|_c = 0 \tag{89}$$

$$\nabla_{\lambda} \mathcal{L}|_c = -\nabla_{\lambda} G|_c \hat{w} + 1 = 0 \tag{90}$$

Based on the OS assumptions, which guarantee that the set of equations (88)-(90) have a unique solution, the full Hessian of the Lagrangian function, i.e. the Jacobian of these equations, must be nonsingular; thus:

$$\nabla^2_{(\hat{z},\hat{\mu},\lambda)} \mathcal{L}(\hat{z}_c, \lambda_c, \hat{p}_o, \hat{w}) \; \rho \neq 0 \quad \forall \rho \neq 0 \tag{91}$$

where

$$\nabla^2_{(\hat{z},\hat{\mu},\lambda)} \mathcal{L}|_c = -\begin{bmatrix} \nabla^2_{\hat{z}} G|_c \hat{w} & \nabla_{\hat{z}} G|_c & \nabla^2_{\lambda\hat{z}} G|_c \hat{w} \\ \nabla^T_{\hat{z}} G|_c & 0 & \nabla^T_{\lambda} G|_c \\ \hat{w}^T \nabla^{2^T}_{\hat{z}\lambda} G|_c & \nabla_{\lambda} G|_c & \nabla^2_{\lambda} G|_c \hat{w} \end{bmatrix} \tag{92}$$

Hence, for a chosen $\rho = (\hat{v}, 0, 0) \neq 0$, from (91) one has that:

$$\left[\nabla^2_{\hat{z}} G|_c \hat{w}\right] \hat{v} \neq 0 \tag{93}$$

since, in this case, $\nabla^{2^T}_{\hat{z}\lambda} G|_c = \nabla^{2^T}_{\lambda\hat{z}} G|_c = 0$. On the other hand, from the second-order KKT necessary optimality conditions [32]:

$$\hat{\rho}^T \; \nabla^2_{(\hat{z},\lambda)} \mathcal{L}|_c \; \hat{\rho} \leq 0 \quad \forall \hat{\rho} \in \mathcal{U}(\hat{z}_c, \lambda_c) \tag{94}$$

where

$$\mathcal{U}(\hat{z}_c, \lambda_c) = \left\{ \hat{\rho} \in \mathbb{R}^{n_{\hat{z}}+1} : [\nabla^T_{\hat{z}} G|_c \; \nabla^T_{\lambda} G|_c] \hat{\rho} = 0 \right\}$$

which implies that $\hat{\rho} = (\hat{v}, 0)$, since $\nabla^T_{\lambda} G|_c$ is a constant nonzero vector. Thus, from (92) and since $\nabla^2_{\lambda} G|_c = 0$ as well, it follows from (94) that:

$$\hat{v}^T \left[\nabla^2_{\hat{z}} G|_c \hat{w}\right] \hat{v} \geq 0$$

Therefore, from (93), it can be concluded that:

$$\hat{v}^T \left[\nabla^2_{\hat{z}} G|_c \hat{w}\right] \hat{v} > 0$$

Finally, taking the transpose of this equation and considering the properties of tensor products:

$$\hat{w}^T \left[\nabla^{2^T}_{\hat{z}} G|_c \hat{v}\right] \hat{v} > 0$$

This corresponds to the third SNB transversality condition (5). ■

APPENDIX III
PROOF OF COROLLARY 1

Proof: Observe that Theorem 1 proofs that an LIDB cannot be a solution of (15). Now, notice that all possible limit conditions of the inequality constraints of (15) are considered in assumptions (16)-(18) and (19)-(20) of Theorems 1 and 2, respectively; thus, the cases of none or all generators reaching their limits are simply particular cases of these assumptions. Hence, any feasible solution of (15), would either meet assumptions (16)-(18) or (19)-(20). Therefore, the solution point $(\hat{z}_c, \lambda_c, \hat{p}_o)$ can only be an LISB or an SNB. ■

REFERENCES

[1] W. D. Rosehart, "Optimal power flows incorporating network stability," in *Proc. IEEE-PES, Winter Meeting*, vol. 2, January 2002, pp. 1100–1104.

[2] G. Irisarri, X. Wang, J. Tong, and S. Mokhtari, "Maximum loadability of power systems using interior point non-linear optimization method," *IEEE Trans. Power Syst.*, vol. 12, no. 1, pp. 162–172, February 1997.

[3] J. Kabouris, C. Vournas, S. Efstathiou, G. Manos, and G. Contaxis, "Voltage security considerations in an open power market," in *Proc. Electric Utility Deregulation and Restructuring and Power Technologies*, April 2000, pp. 278–283.

[4] "Voltage stability assesment: Concepts, practices and tools," IEEE/PES Power System Stability Subcommittee, Tech. Rep. SP101PSS, August 2002.
[5] C. A. Cañizares, N. Mithulananthan, F. Milano, and J. Reeve, "Linear performance indices to predict oscillatory stability problems in power systems," *IEEE Trans. Power Syst.*, vol. 19, no. 2, pp. 1104–1114, May 2004.
[6] W. Marszalek and Z. W. Trzaska, "Singularity-induced bifurcations in electrical power systems," *IEEE Trans. Power Syst.*, vol. 20, no. 1, pp. 312–320, February 2005.
[7] R. Riaza, S. L. Campbell, and W. Marszalek, "On singular equilibria of index-1 DAEs," *Circuits Systems Signal Process*, vol. 19, no. 2, pp. 131–157, 2000.
[8] V. Ajjarapu and C. Christy, "The continuation power flow: A tool for steady state voltage stability analysis," *IEEE Trans. Power Syst.*, vol. 1, no. 1, pp. 416–423, February 1992.
[9] C. A. Cañizares and F. L. Alvarado, "Point of collapse and continuation methods for large ac/dc systems," *IEEE Trans. Power Syst.*, vol. 8, no. 1, pp. 1–8, February 1993.
[10] C. A. Cañizares, "Calculating optimal system parameters to maximize the distance to saddle-node bifurcations," *IEEE Trans. Circuits Syst. I*, vol. 3, no. 45, pp. 225–237, March 1998.
[11] T. Van Cutsem, "A method to compute reactive power margins with respect to voltage collapse," *IEEE Trans. Power Syst.*, vol. 6, no. 1, pp. 145–155, February 1991.
[12] E. Vaahedi, Y. Mansour, C. Fuchs, S. Granville, M. D. L. Latore, and H. Hamadanizadeh, "Dynamic security constrained optimal power flow/var planning," *IEEE Trans. Power Syst.*, vol. 16, no. 1, pp. 38–43, February 2001.
[13] F. Milano, C. A. Cañizares, and M. Invernizzi, "Multi-objective optimization for pricing system security in electricity markets," *IEEE Trans. Power Syst.*, vol. 18, no. 2, pp. 596–604, May 2003.
[14] W. D. Rosehart, "Optimization of power systems with voltage security constraints," Ph.D. dissertation, University of Waterloo, Waterloo, ON. Canada, 2000.
[15] W. D. Rosehart, C. A. Cañizares, and V. H. Quintana, "Multiobjective optimal power flows to evaluate voltage security cost in power networks," *IEEE Trans. Power Syst.*, vol. 18, no. 2, pp. 578–587, May 2003.
[16] G. L. Torres and V. H. Quintana, "An interior point method for nonlinear optimal power flow using voltage rectangular coordinates," *IEEE Trans. Power Syst.*, vol. 13, no. 4, pp. 1211–1218, November 1998.
[17] W. Rosehart, C. Roman, and A. Schellenberg, "Optimal power flow with complementarity constraints," *IEEE Trans. Power Syst.*, vol. 20, no. 2, pp. 813–822, May 2005.
[18] C. D. Vournas, M. Karystianos, and N. G. Maratos, "Bifurcation points and loadability limits as solutions of constrained optimization problems," in *Proc. IEEE-PES, Summer Meeting*, vol. 3, July 2000, pp. 1883–1888.
[19] M. E. Karystianos, N. G. Maratos, and C. D. Vournas, "Maximizing power-system loadability in the presence of multiple binding complementarity constraints," *IEEE Trans. Circuits Syst.*, vol. 54, no. 8, pp. 1775–1787, August 2007.
[20] N. G. Maratos and C. D. Vournas, "Relationships between static bifurcations and constrained optima," in *ISCAS 2000*, vol. 2, Geneva, Switzerland, May 2000, pp. 477–480.
[21] P. Kundur *et al.*, "Definition and clasification of power system stability," *IEEE Trans. Power Syst.*, vol. 19, no. 2, pp. 1387–1401, May 2004.
[22] P. Kundur, *Power System Stability and Control*, ser. Power System Engineering. McGraw-Hill, 1994.
[23] D. J. Hill and I. M. Y. Mareels, "Stability theory for differential/algebraic systems with application to power systems," *IEEE Trans. Circuits Syst.*, vol. 37, no. 11, pp. 1416–1423, November 1990.
[24] V. Venkatasubramanian, H. Schättler, and J. Zaborszky, "A taxonomy theory of the dynamics of large power systems with emphasis on its voltage stability," in *Bulk Power System Voltage Phenomena II-Voltage Stability and Security*, L. H. Fink, Ed., August 1991, pp. 9–52.
[25] I. Dobson, "Observations on the geometry of saddle node bifurcations and voltage collapse in electrical power systems," *IEEE Trans. Circuits Syst. I*, vol. 39, no. 3, pp. 240–243, March 1992.
[26] C. A. Cañizares, "Conditions for saddle-node bifurcations in ac/dc power systems," *International Journal of Electrical Power and Energy Systems*, vol. 17, no. 1, pp. 61–68, January 1995.
[27] R. Seydel, *Practical Bifurcation and Stability Analysis: from equilibrium to chaos*, 2nd ed. Springer-Verlag, 1994.
[28] I. Dobson and H. D. Chiang, "Towards a theory of voltage collapse in electric power systems," *Systems & Control Letters*, vol. 13, pp. 253–262, 1989.
[29] I. Dobson and L. Lu, "Voltage collapse precipitated by the immediate change in stability when generator reactive power limits are encountered," *IEEE Trans. Circuits Syst. I*, vol. 39, no. 9, pp. 762–766, September 1992.
[30] V. Venkatasubramanian, H. Schättler, and J. Zaborszky, "Dynamics of large constrained nonlinear systems-a taxonomy theory," in *Proceedings of the IEEE*, vol. 83, no. 11, November 1995, pp. 1530–1560.
[31] H. Y. Benson, D. F. Shanno, and R. J. Vanderbei, "Interior-point methods for nonconvex nonlinear programming: Complementarity constraints," *Operations Research and Financial Engineering*, pp. 1–20, September 2002.
[32] J. Nocedal and S. J. Wright, *Numerical Optimization*. Springer, 1999.
[33] C. A. Cañizares, F. L. Alvarado, C. L. DeMarco, I. Dobson, and W. F. Long, "Point of collapse methods applied to ac/dc power systems," *IEEE Trans. Power Syst.*, vol. 2, no. 7, pp. 673–683, May 1992.
[34] R. Fourer, D. M. Gay, and B. W. Kernighan, *AMPL A Modeling Language for Mathematical Programming*, 2nd ed. Thomson, 2003.
[35] M. C. Ferris, R. Fourer, and D. M. Gay, "Expressing complementarity problems in an algebraic modeling languange and communicating them to solvers." [Online]. Available: www.ampl.com
[36] "KNITRO." [Online]. Available: http://www.ziena.com
[37] C. A. Cañizares et. al, "UWPFLOW." [Online]. Available: http://thunderbox.uwaterloo.ca/ claudio/software/pflow.html
[38] F. Zhang, *The Schur Complement and Its Applications*. Springer, 2005.
[39] E. Castillo, A. J. Conejo, C. Castillo, R. Mínguez, and D. Ortigosa, "Perturbation approach to sensitivity analysis in mathematical programming," *J. Optimization Theory and Applications*, vol. 128, no. 1, p. 49–74, January 2006.

Rafael J. Avalos (SM'97) received his M.Sc. degree (2004) in Electrical Engineering from the Instituto Tecnológico de Morelia, México. He is currently a PhD Student at the Electrical Department of the University of Waterloo, Canada. His research interests include the analysis and application of optimization techniques to stability-constrained OPFs in a electricity market environment.

Claudio A. Cañizares (S'85, M'91, SM'00, F'07) received in April 1984 the Electrical Engineer diploma from the Escuela Politécnica Nacional (EPN), Quito-Ecuador, where he held different teaching and administrative positions from 1983 to 1993. His MS (1988) and PhD (1991) degrees in Electrical Engineering are from the University of Wisconsin-Madison. Dr. Cañizares has held various academic and administrative positions at the E&CE Department of the University of Waterloo since 1993, where he is currently a Full Professor. His research activities concentrate on the study of modeling, simulation, control, stability and computational issues in power systems in the context of competitive electricity markets.

Federico Milano (M'03) received the M.S. degree and the Ph.D. degree in 1999 and 2003, respectively, from the Università di Genova, Italy. In 2001-2002 he was a Visiting Scholar at the University of Waterloo, ON, Canada. He is currently an Associate Professor at the Universidad de Castilla-La Mancha, Ciudad Real, Spain. His research interests include voltage stability, electricity markets and computer-based power system modeling.

Antonio J. Conejo (F'04) received the M.S. degree from MIT, Cambridge, MA, in 1987, and a Ph.D. degree from the Royal Institute of Technology, Stockholm, Sweden in 1990. He is currently a full Professor at the Universidad de Castilla-La Mancha, Ciudad Real, Spain. His research interests include control, operations, planning and economics of electric energy systems, as well as statistics and optimization theory and its applications.